

## Observation of ordered oxygen vacancies on $\text{TiO}_2(100)1 \times 3$ using scanning tunneling microscopy and spectroscopy

P. W. Murray, F. M. Leibsle, H. J. Fisher,\* C. F. J. Flipse,<sup>†</sup> C. A. Muryn,\* and G. Thornton\*  
*Interdisciplinary Research Centre in Surface Science, University of Liverpool, Liverpool L69 3BX, United Kingdom*  
 (Received 27 July 1992)

Scanning tunneling microscopy (STM) and spectroscopy have been used to investigate the structure of rutile  $\text{TiO}_2(100)1 \times 3$ . The combination of these two techniques allows us to identify individual oxygen vacancies on the  $1 \times 3$  reconstructed surface. These vacancies are found to occupy the topmost layer of the surface and to form one-dimensional arrays in the  $[001]$  crystallographic direction, with an intervacancy separation of 2.96 Å and a typical length of  $\sim 500$  Å. The STM data are consistent with a microfacet structural model proposed on the basis of grazing incidence x-ray diffraction data, modified to include the presence of O vacancies in the top layer.

Oxygen vacancies in the bulk and at the surface of metal oxides are thought to fundamentally alter physical and chemical properties.<sup>1,2</sup> Such properties play a key role in the technological applications of oxides, for instance, in ceramic fracture, catalytic reactions, and photovoltaic devices. Although much is known about the structure of vacancies in the bulk materials,<sup>1</sup> there is little experimental data relating to the surface structure.<sup>2</sup> In this paper we report the study of O-vacancy structure on a reduced (100) surface of rutile  $\text{TiO}_2$  using scanning tunneling microscopy (STM) and spectroscopy (STS) in ultrahigh vacuum (UHV).

The surfaces of  $\text{TiO}_2$  have been the subject of a number of theoretical<sup>3,4</sup> and experimental studies.<sup>4-10</sup> STM work has included the study of a reduced (110) surface of rutile  $\text{TiO}_2$ ,<sup>5</sup> in which atomic resolution was achieved. The complex structures observed were ascribed to the formation of O-vacancy-induced crystallographic shear planes<sup>5</sup> which surprisingly are apparently unrelated to the surface structures derived from diffraction techniques.<sup>6</sup> More recently, an STM study of the (100) surface observed a tripling of the bulk-terminated surface unit-cell constant in the  $[010]$  direction,<sup>7</sup> consistent with the  $1 \times 3$  reconstruction observed by low-energy electron diffraction (LEED).<sup>8,9</sup>

Consistent with photoemission data, which evidence O-vacancy creation accompanying the reconstruction,<sup>9</sup> a simple model was proposed for the  $1 \times 3$  surface which involves the removal of every third  $[001]$ -direction row of O atoms. A more complex, microfacet model has recently been deduced from grazing incidence x-ray diffraction (GXR) data which contain facets of the lowest-energy, (110) plane.<sup>10</sup> Since a stoichiometric termination was assumed, in line with an early study,<sup>5</sup> O atoms are placed in the topmost layer of this model.<sup>10</sup> Removing these atoms provides a means of incorporating oxygen vacancies into the microfacet structure, making the model consistent with photoemission data.<sup>9</sup> This is the structure indicated by our STM (S) results, in which individual O vacancies are identified. These vacancies are found to form one-dimensional arrays of typical length  $\sim 500$  Å in the  $[001]$  direction.

Our STM (S) measurements employed an Omicron

UHV instrument operated at a base pressure of  $\leq 10^{-10}$  mbar. In this instrument, which is designed for room-temperature measurements, the (tungsten) tip is held at ground potential and the sample is biased. Imaging was carried out in the constant-height, constant-current, and spectroscopy modes. During constant-height scans the time constant of the feedback loop is increased, keeping the tip a constant distance above the surface. The image is formed from variations in the tunneling current and not the vertical height movement of the tip as in constant-current images. Spectroscopy data were recorded by measuring the  $I$ - $V$  characteristics for each pixel of the topographic image by temporarily breaking the feedback loop at each pixel, thus freezing the tip a fixed distance from the surface, while ramping the voltage between the sample and tip.

The two samples used were cut from the same boule (Commercial Crystals Inc.) One sample was cut and polished ( $0.25 \mu\text{m}$ ) to within  $0.25^\circ$  of the (100) plane while the other was cut and polished  $2.6^\circ \pm 0.1^\circ$  off the (100) plane towards  $[001]$  as determined by Laue diffraction.<sup>11</sup> Samples were vacuum reduced to introduce  $n$ -type conductivity (ca.  $10^{18} \text{ cm}^{-3}$ ) and cleaned *in situ* by cycles of Ar-ion bombardment and annealing to 870 K, following an established technique to form a clean  $1 \times 3$  reconstructed surface.<sup>9</sup> LEED was used to check the macroscopically averaged symmetry of the surfaces.

Figure 1 shows a constant-current image of the  $1 \times 3$  vicinal surface obtained at positive sample bias.<sup>12</sup> We first focus on the rows parallel to  $[001]$ , which typically run along wide (ca. 500 Å) terraces to terminate in irregular step edges. The image contains elements of topographic features generally present on the surface. In particular, irregularly spaced, rough-edged steps (*A*) are seen in the  $[010]$  vicinal off-cut direction. More regular steps (*B*) are observed in the perpendicular direction, i.e., with step edges parallel to  $[001]$ , as expected on the basis of LEED data.<sup>9</sup> We found that atomic resolution along the bright rows, as seen in Fig. 2, could only be achieved by employing the constant-height mode of scanning. This scan mode has the advantage that images can be obtained much faster, minimizing thermal drift effects. Current profiles between and along the rows indicate a surface

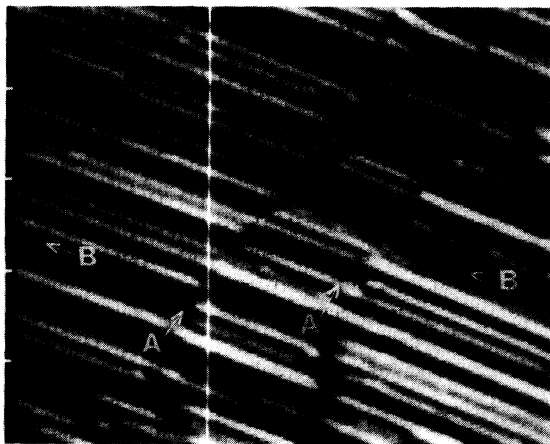


FIG. 1. A  $500 \times 600 \text{ \AA}^2$  constant-current ( $+2.0 \text{ V}$ ,  $0.2 \text{ nA}$ ) image of the vicinal  $\text{TiO}_2(100)1 \times 3$  surface. The tick marks along the vertical axis are spaced by  $100 \text{ \AA}$ , and the length scales have not been corrected. In this image, which has been post-differentiated to highlight topographic features, the  $[001]$  direction corresponds to the bright rows.

unit cell of dimensions  $3.3 \times 15.4 \text{ \AA}^2$ ,<sup>13</sup> with a corrugation of  $0.06 \text{ nA}$  along the rows at  $+2\text{-V}$  bias. These cell dimensions compare with those expected for a  $1 \times 3$  unit cell of  $2.96 \times 13.77 \text{ \AA}^2$ . The discrepancy can be associated with instrumental factors such as thermal drift and piezoelectric creep. By comparing the ratio of the cell lengths we can avoid most of these problems, resulting in very close agreement between the STM-derived value, 4.72, and that expected from the bulk cell constants, 4.70. This validates our assertion that we are imaging atoms on the surface and that we can pinpoint the  $1 \times 3$  unit cell.



FIG. 2. A  $30 \times 40 \text{ \AA}^2$  constant-height image of the planar  $\text{TiO}_2(100)1 \times 3$  surface, with the tip stabilized at  $+2 \text{ V}$  sample bias and  $0.2 \text{ nA}$  tunneling current before disengaging the feedback loop. The image, in which the rows lie parallel to the  $[001]$  direction, is displayed as a tilted, three-dimensional figure for ease of viewing. The  $1 \times 3$  unit cell is marked on the image which terminates in structure along the rows which we associate with Ti atom positions. The length scales have not been corrected.

We identify Ti atoms with the features on the atomic rows in Fig. 2 by reference to STS data. Figure 3(a) shows STS spectra recorded with the STM tip on and between the rows seen in Fig. 2. It is clear that there is a considerable difference in the contribution to the tunneling current in the two positions, with little tunneling current at negative sample bias when the tip is on the rows. The corresponding differential conductance spectra, which provide a representation of the local density of states (DOS),<sup>14</sup> are shown in Fig. 3(b) where they are compared with calculations of the surface electronic structure.<sup>3</sup> Munnix and Schmeits have calculated layer DOS for the three possible bulk terminations of  $\text{TiO}_2(100)$ . In Fig. 3(b) we use their results for a Ti-terminated surface, comparing the differential conductance spectra with the layer DOS for top layer Ti atoms and second layer O atoms. A comparison of the two calculated DOS illustrates the point that in this relatively ionic material oxygen atoms provide most of the contribution to the occupied states near the Fermi level, while Ti atoms provide the unoccupied states. That the on-row differential conductance spectrum indicates a relatively small occupied DOS provides compelling evidence that the rows are composed of oxygen vacancies.

We can now also explain why the successful imaging of this surface was only accomplished with positive sample bias conditions. The spectroscopy curves of Fig. 3 show that on the bright rows very little tunneling current occurs in the negative bias region. When the STM is operated in the constant-current mode with negative bias this will probably result in a tip crash. Alternatively, the tip will approach sufficiently close to the sample to cause field-induced desorption or deposition, both of which would result in damage to the surface.

We turn now to the relationship between the O-vacancy structure and the microfacet model. An obvious discrepancy arises from the lack of O vacancies in the microfacet model deduced from GXR D,<sup>10</sup> which presumably arises from the relative insensitivity of GXR D to oxygen atoms. We start from the proposition that these O

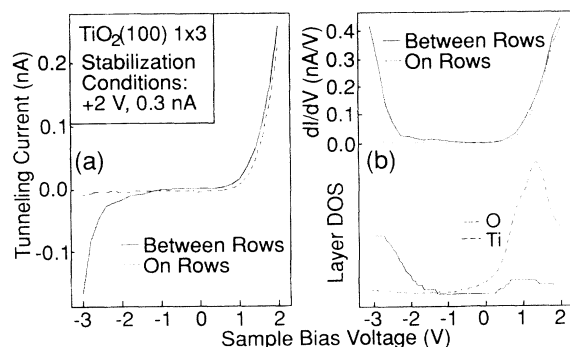


FIG. 3. (a) STS spectra obtained on and between the bright rows seen in Fig. 1. (b) The corresponding differential conductance spectra compared with the calculated layer DOS for top-layer Ti atoms and second-layer O atoms of  $\text{TiO}_2(100)$  (from Ref. 3). The calculated DOS have been rigidly shifted to align them with experiment at the center of the band gap. The experimental band gap is consistent with the optical band gap of  $3.05 \text{ eV}$ .

vacancies (Ti atoms) lie in the topmost layer of a microfacet model, as shown in Fig. 4, giving Ti atoms a threefold coordination to oxygen. To test this idea we compare, in Fig. 4, an STM height profile recorded perpendicular to the rows observed in Figs. 1 and 2 with a structural model. Here we have deliberately chosen to include a step in the linear scan and model. The measured value of the step height obtained from the peak heights on either side of the step is  $4.6 \text{ \AA}$ , in excellent agreement with that expected for a step of height  $4.59 \text{ \AA}$ , corresponding to one unit cell along the surface normal.

The height profile indicates that the depth of a microfacet on the terrace is  $\sim 3 \text{ \AA}$  as compared to  $\sim 5 \text{ \AA}$  for the model. This  $2\text{-\AA}$  discrepancy is also reflected in the depth of the microfacet on the step ( $\sim 7 \text{ \AA}$  as opposed to  $\sim 9 \text{ \AA}$  from the model). Such discrepancies might be expected to arise from variations in the tunneling geometry and electronic structure; however, they raise the question of whether the height profiles reveal more about the electronic structure than the geometric structure of the reconstruction. Returning to the step structure, we first note that its model in Fig. 4 is entirely consistent with the microfacet structure, representing a continuation of a (110) facet. On this basis, the height profile over the step edge supports the proposition that O vacancies occupy the top layer, in that the gradient at the step edge is similar to that of the microfacets. This would not be expected if O vacancies occupied sites at the bottom, or sides of the facets, with an apparently greater height in STM images arising from the tunneling conditions.

In summary, we have identified individual O vacancies on  $\text{TiO}_2(110)1 \times 3$  using a combination of STM and STS. The STM data are entirely consistent with a microfacet structural model proposed from x-ray diffraction data, modified to include the presence of O vacancies in the top layer. This modification of the model makes it consistent with photoemission data, which evidence Ti  $3d$  states  $\sim 1 \text{ eV}$  below the conduction-band minimum. That these

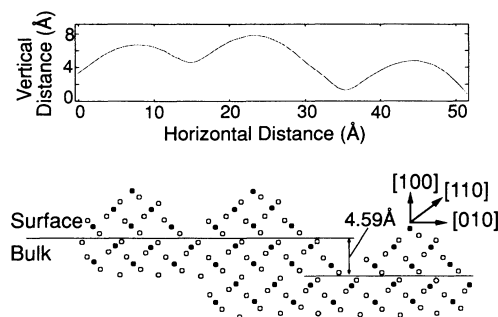


FIG. 4. In the upper part of the diagram is shown an STM height profile of the planar  $1 \times 3$  surface in the [010] direction across a step. The height (Ref. 13) and horizontal scales have been adjusted, the latter by a reduction of  $\sim 10\%$  to line up the peaks of the line scan and model. This reduction corresponds to the discrepancy noted in the unit cell dimensions obtained from the image in Fig. 2. The lower part of the diagram shows to the same scale a modified microfacet model (from Ref. 10) viewed along [001], where Ti (O) atom positions are represented by filled (open) symbols. The model has been modified to remove top-layer O atoms and to include step structure which is a continuation of a (110) facet.

states are not distinguished in our STS spectra may reflect their polaronic character<sup>15</sup> or be in some way associated with the one-dimensional character of Ti-Ti bonding along the rows. This work indicates that STM (S) holds considerable promise in the study of surface defect formation on oxides by relating images to the results of other structural techniques.

This work was funded by the United Kingdom Science and Engineering Research Council with additional support from Harwell Laboratory.

\*Also at Chemistry Department, Manchester University, Manchester M13 9PL, UK.

†Present address: Technische Universiteit Eindhoven, Postbus 513, 5600MB Eindhoven, The Netherlands.

<sup>1</sup>A. De Vita, M. J. Gillan, J. S. Lin, M. C. Payne, I. Stich, and L. J. Clarke, *Phys. Rev. Lett.* **68**, 3319 (1992).

<sup>2</sup>E. A. Colbourn, *Surf. Sci. Rep.* **15**, 281 (1992).

<sup>3</sup>S. Munnix and M. Schmeits, *Phys. Rev. B* **30**, 2202 (1984).

<sup>4</sup>V. E. Henrich, in *Surface and Near-Surface Chemistry of Oxide Materials*, edited by J. Nowotny and L.-C. Dufour (Elsevier, Amsterdam, 1988), p. 23.

<sup>5</sup>G. S. Rohrer, V. E. Henrich, and D. A. Bonnell, *Science* **250**, 1239 (1990).

<sup>6</sup>B. L. Maschhoff, J.-M. Pan, and T. E. Madey, *Surf. Sci.* **259**, 190 (1991).

<sup>7</sup>G. W. Clarke and L. L. Kesmodel, *Ultramicroscopy* **41**, 77 (1992).

<sup>8</sup>Y. W. Chung, W. J. Lo, and G. A. Somorjai, *Surf. Sci.* **64**, 588 (1977).

<sup>9</sup>C. A. Muryn, P. J. Hardman, J. J. Crouch, G. N. Raikar, G. Thornton, and D. S.-L. Law, *Surf. Sci.* **251**, 747 (1991).

<sup>10</sup>P. Zschack, J. B. Cohen, and Y. W. Chung, *Surf. Sci.* **262**, 395 (1991).

<sup>11</sup>A vicinal sample was used to allow us to carry out a parallel investigation of the step structure.

<sup>12</sup>As in the earlier study of  $\text{TiO}_2(110)$  (Ref. 5), we were not able to reproducibly image the surface with negative sample bias voltages.

<sup>13</sup>Calibration of the STM employed images from a vicinal  $\text{Si}(111)7 \times 7$  surface.

<sup>14</sup>M. Tsukada, K. Kobayashi, N. Isshiki, and H. Kageshima, *Surf. Sci. Rep.* **13**, 265 (1991).

<sup>15</sup>R. G. Egdell, S. Eriksen, and W. R. Flavell, *Solid State Commun.* **60**, 835 (1986).

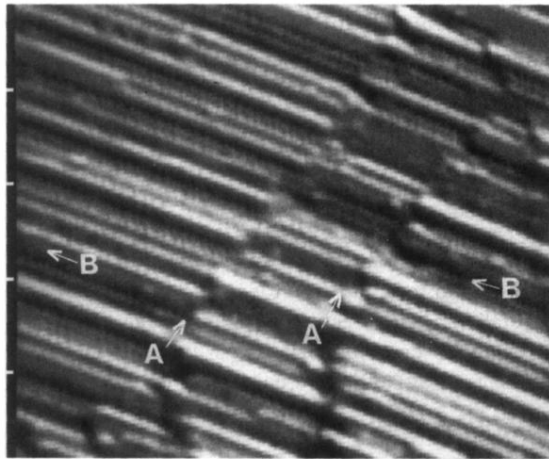


FIG. 1. A  $500 \times 600 \text{ \AA}^2$  constant-current (+2.0 V, 0.2 nA) image of the vicinal  $\text{TiO}_2(100)1 \times 3$  surface. The tick marks along the vertical axis are spaced by  $100 \text{ \AA}$ , and the length scales have not been corrected. In this image, which has been post-differentiated to highlight topographic features, the [001] direction corresponds to the bright rows.

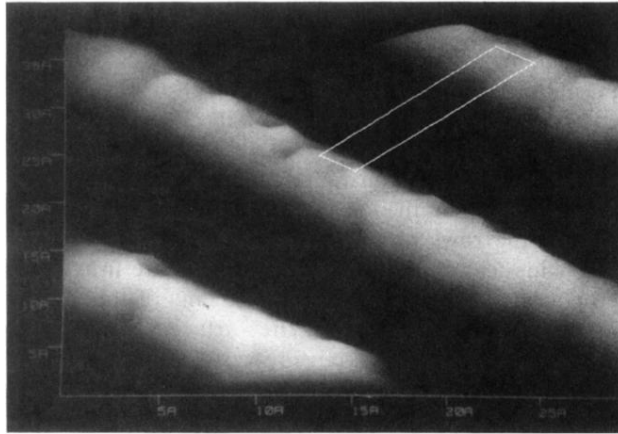


FIG. 2. A  $30 \times 40 \text{ \AA}^2$  constant-height image of the planar  $\text{TiO}_2(100)1 \times 3$  surface, with the tip stabilized at +2 V sample bias and 0.2 nA tunneling current before disengaging the feedback loop. The image, in which the rows lie parallel to the [001] direction, is displayed as a tilted, three-dimensional figure for ease of viewing. The  $1 \times 3$  unit cell is marked on the image which terminates in structure along the rows which we associate with Ti atom positions. The length scales have not been corrected.